ENGINEERING TRANSACTIONS • *Engng. Trans.* • **43**, 4, 553–569, 1995
Polish Academy of Sciences • Institute of Fundamental Technological Research

CYCLIC LOADING OF A NOTCHED ELEMENT WITH A TECHNOLOGICAL SURFACE LAYER

S. KUCHARSKI (WARSZAWA)

A method for determining the stresses in a notched element with a technological surface layer (TSL) subjected to low-cycle loading is presented. The considerations are based on the kinematic-isotropic model of strain hardening and the theory of plastic flow. The hysteresis loops obtained for a specimen with and without a surface layer, under the same loading conditions are compared with each other. The same is done for the working and residual stresses for a specimen with a surface layer.

1. INTRODUCTION

The surface layer of a machine element is, in view of its importance for the strength and the life of the latter, the subject of experimental studies of increasing intensity. At the same time theoretical models of elements with a TSL are devised and tested with a view to obtain a means for determining the equivalent stress distribution for the entire element, the influence of the presence of the TSL being taken into consideration and, in particular, for the surface layer itself. Elements with a TSL subjected to elastic-plastic strain are usually modelled by methods of finite elements, as was done for instance in papers [1, 2 and 3], devoted to problems of contact loads acting on an element with a surface layer, such as the problem of state of stress produced by various rigid indenters. The surface layer was modelled in those works by taking finite elements of the same type as those used for the core, but of finer dimensions. The residual stresses and the roughness of the surface layer were not taken into account. It was assumed to be homogeneous, its elastic-plastic properties being different, however, from those of the core. Only monotonic loads were considered on the basis of the theory of plastic flow assuming isotropic strain hardening. However, experimental investigation shows that the TSL is very important in the case of cyclic loading. A solution to the problem of cyclic (compression-tension) loading has been presented in [4] for a cylinder with a TSL. It has been obtained by applying the theory of

plastic flow and the isotropic model of strain hardening, the surface layer being modelled as a thin membrane in a plane state of stress.

The algorithm which will be presented below and has been devised for determining the state of stress in an element with a TSL, subjected to cyclic loading, is based of the method of finite elements. The theory of plastic flow will be used assuming small elastic-plastic strain and a mixed type (kinematic and isotropic) model of strain hardening. The program for the finite element procedure is confined to plane and axially symmetric problems and a type of loading as that used for fatigue tests (tension and torsion), without considering contact loads. The model of the layer will be assumed in the form of a thin membrane, similarly to [4, 5] and [6], the initial stresses being taken into consideration. Finally, an example of application of the program for determining the state of stress in a specimen with a notch and a TSL will be presented.

2. The constitutive model

The model assumed is based on the theory of plastic flow taking into account kinematic and isotropic strain hardening [7, 8]. The moduli of kinematic and isotropic strain hardening are not constant, but depend on the plastic strain (or, in a multi-axial state of stress, on the length of the trajectory in the space of plastic strain). The yield condition is assumed in the form

$$F(\sigma, \alpha, \bar{\varepsilon}_p) = f(\sigma - \alpha) - Y(\bar{\varepsilon}_p) = 0, \tag{2.1}$$

where σ – stress tensor, α – stress tensor determining the translation of the centre of the yield surface (the coordinate of the centre of the elastic region in uniaxial state of stress), $\bar{\varepsilon}_p$ – length of the trajectory in the space of plastic strain, $Y(\bar{\varepsilon}_p)$ – measure of expansion of yield surface when $\bar{\varepsilon}_p = 0$.

The evolutions of the variables of state α and Y (the yield point) will be taken into consideration as functions of the evolution parameter $\bar{\varepsilon}^p$. Those functions are treated as input data of the algorithm and are given in a tabulated form. They can be obtained from a test of uniaxial cyclic compression and tension. In the case of cyclic load they are usually represented as a hysteresis loop of stress and a hysteresis loop of the parameter α, cf. Fig. 1 [9]. In such a representation, the parameter $\bar{\varepsilon}^{p^*}$ (which is marked on the abscissa axis) may assume negative values because it is equal to the plastic strain for compression or tension and, according to the above definition of $\bar{\varepsilon}^p$, it is a

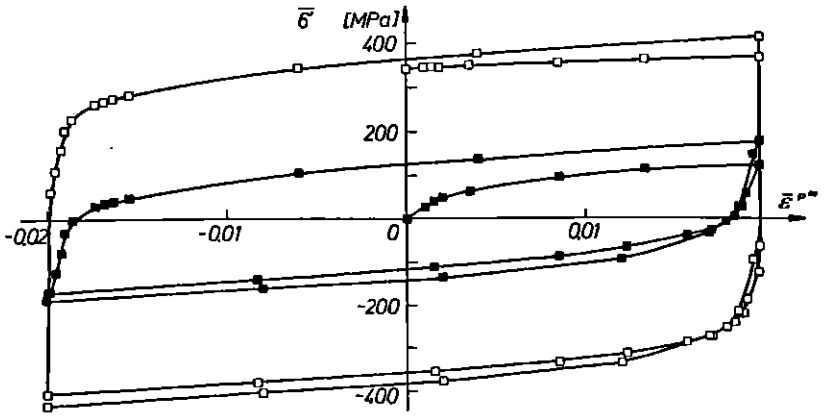

FIG. 1. Cyclic curves of total and kinematic strain-hardening.

sum of the absolute values of $\bar{\varepsilon}^{p*}$ obtained for alternating compression and tension of the specimen.

The total strain-hardening is a sum of kinematic and isotropic strain-hardening. The curves expressing those quantities under a monotonic load are represented (at the beginning of the hysteresis loop) in Fig. 2.

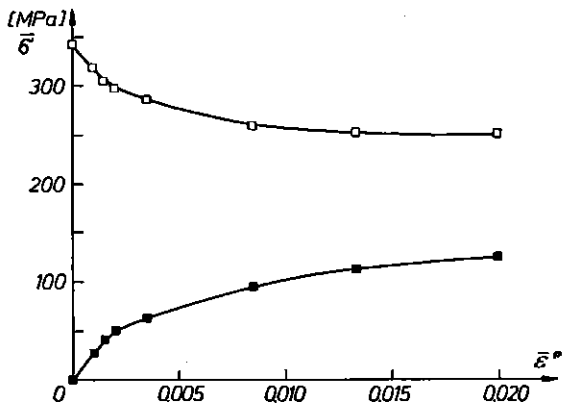

FIG. 2. Curves of isotropic and kinematic strain-hardening for monotonic tension.

From experiments which were conducted for steel [9] it follows that in the case of a cyclic load, the curve of isotropic strain hardening descends in a monotonic manner and becomes stable after no more than a few load cycles, the total strain-hardening being decided upon by only the kinematic strain-hardening (the curve of the variable α, Fig. 1).

Making use of the yield condition (2.1), the compatibility condition can be thus expressed by

$$\frac{\partial f(\sigma-\alpha)}{\partial \sigma}\cdot d\sigma - H^* d\lambda = 0, \tag{2.2}$$

where H^* is the total modulus of strain hardening, that is the sum of the kinematic and isotropic strain-hardening modulus, H^α and H^I, respectively,

$$H^* = H^\alpha + H^I. \tag{2.3}$$

Equation (2.2) may be rewritten in the form

$$\frac{\partial f(\sigma-\alpha)}{\partial \sigma}\cdot d\sigma + \frac{\partial f(\sigma-\alpha)}{\partial \alpha}\cdot d\alpha - \frac{dY}{d\bar{\varepsilon}^p} d\bar{\varepsilon}^p = 0. \tag{2.4}$$

Assuming that $\bar{\varepsilon}^p = \lambda$, we have

$$H^* d\lambda = \frac{\partial f(\sigma-\alpha)}{\partial \alpha}\cdot d\alpha - \frac{dY}{d\lambda} d\lambda. \tag{2.5}$$

We shall now use the Zigler equation describing the evolution of variable α

$$d\alpha = d\mu(\sigma-\alpha), \tag{2.6}$$

where μ is a function of λ. On denoting

$$\frac{d\mu}{d\lambda} = c, \tag{2.7}$$

c being a constant or function of λ, we have

$$d\alpha = c d\lambda(\sigma-\alpha). \tag{2.8}$$

Taking into account the relations (2.6) to (2.8) we obtain from (2.4)

$$\frac{\partial f(\sigma-\alpha)}{\partial \sigma}\cdot d\sigma + \left(c\frac{\partial f(\sigma-\alpha)}{\partial \alpha}\cdot(\sigma-\alpha) - H^I\right) d\lambda = 0. \tag{2.9}$$

By confronting (2.2), (2.4) and (2.9), we find

$$H^\alpha = c\frac{\partial f(\sigma-\alpha)}{\partial \alpha}\cdot(\sigma-\alpha), \tag{2.10}$$

$$H^I = \frac{dY(\bar{\varepsilon}^p)}{d\lambda}. \tag{2.11}$$

From (2.9), (2.10) and (2.11) it is seen that the modulus of kinematic strain hardening is decisive for the velocity of displacement of the yield surface and the modulus of isotropic strain hardening – for the variation rate of the radius of that surface.

If H_α is treated as a prescribed quantity, the quantity c can be eliminated from Eqs. (2.7) and (2.10), and $d\mu$ can be expressed by the formula

$$d\mu = \frac{H^\alpha d\lambda}{\dfrac{\partial f(\sigma-\alpha)}{\partial \alpha}\cdot(\sigma-\alpha)}. \tag{2.12}$$

The remaining equations used with our algoritm will be expressed in an incremental form convenient for use with a program based on the method of finite elements. It is assumed that the total strain is a sum of plastic and elastic strain, that is

$$d\varepsilon = d\varepsilon^e + d\varepsilon^p . \tag{2.13}$$

From Hooke's law we have

$$d\sigma = \mathbf{D}\cdot d\varepsilon^e, \tag{2.14}$$

where $\mathbf{D}$ is the elasticity matrix and from the flow law

$$d\varepsilon^p = d\lambda \frac{\partial f(\sigma - \alpha)}{\partial \sigma}, \tag{2.15}$$

we obtain the fundamental incremental equation of calculation procedure

$$d\sigma = \mathbf{D}(d\varepsilon - d\varepsilon^p) = \mathbf{D}\cdot\left(d\varepsilon - d\lambda \frac{\partial f}{\partial \sigma}\right). \tag{2.16}$$

Making use of (2.16) and (2.4) we can find $d\lambda$:

$$d\lambda = \frac{\mathbf{d}^T \cdot d\varepsilon}{H^* + \dfrac{\partial f^T(\sigma - \alpha)}{\partial \sigma}\cdot \mathbf{d}}, \tag{2.17}$$

where

$$\mathbf{d}^T = \frac{\partial f^T(\sigma - \alpha)}{\partial \sigma}\cdot \mathbf{D}. \tag{2.18}$$

By analysing Eqs. (2.2) to (2.18) we conclude that, knowing the functions $H^I(\lambda)$, $(H^I(\bar{\varepsilon}^p))$ and $H^\alpha(\lambda)$, $(H^\alpha(\bar{\varepsilon}^p))$, we can determine by incremental means all the unknown quantities involved.

3. Implementation of the model in a FEM-system

In programs based on the method of finite elements (FEM), the algorithm of the procedure of integrating the equations of plasticity can be described in the following simplified form:

- The establishment of the load increment (the load being applied by consecutive steps), further referred to as increments.
- The determination of the increment of the strain tensor as a result of an increment of the prescribed load.

• The determination of the elastic increment of the stress tensor $\Delta\sigma = \mathbf{D}\Delta\varepsilon$ connected with the increment of strain.

• The reduction of the stresses place them to the current yield surface. This step take place if, after addition of the previously calculated increment $\Delta\sigma$, the values of the stress components are such that the point in the space of the stresss is situated outside the surface. The current yield surface is determined taking into consideration its extension $dY(\bar{\varepsilon}_p)$ and its displacement $d\alpha$ resulting from the last increase in stress. To determine the increments of the quantities (σ, ε) connected with the return to the yield surface several iterations are performed, the number of which depends on the required accuracy.

The above algorithm is repeated for each increment of the load. The procedure assumed is similar to that of [10] and is completed by some terms resulting from two types of strain hardening. Below we shall quote the particular equations which have been used with the above algorithm. It should be borne in mind that the quantity controlling the entire process is the increment of the load.

The known functions $H^I(\bar{\varepsilon}^p)$ and $H^\alpha(\bar{\varepsilon}^p)$ are assumed to be piecewise linear, the boundary points between the segments being denoted $\bar{\varepsilon}^p_1, \bar{\varepsilon}^p_2, \ldots, \bar{\varepsilon}^p_k, \bar{\varepsilon}^p_{k+1}$. Owing to this assumption, any experimental curve can be easily approximated, the strain-hardening moduli are constant over consecutive intervals of $\bar{\varepsilon}^p$ and, for instance, the moduli of total strain-hardening, H^*, can be determined directly from uniaxial yield test according to the formula

$$H^*_k = \frac{Y_{k+1} - Y_k}{\bar{\varepsilon}^p_{k+1} - \bar{\varepsilon}^p_k}, \tag{3.1}$$

where Y_k are the values of the stress on the $\sigma - \varepsilon$ curve, and $\bar{\varepsilon}^p_k$ – the relevant values of plastic strain. Making use of the formulae derived above, the consecutive steps of the above algorithm for integration of the equations of plasticity can be easily described as follows (we assume that the procedure starts from certain fixed values σ^u, α^u, $\bar{\varepsilon}^{pu}$, which have already been calculated by the same algorithm, and we are concerned with the next increment of the load). We determine

1. The elastic increment of stress

$$\Delta\sigma = \mathbf{D}\Delta\varepsilon, \tag{3.2}$$

and the assumed new value of the stress tensor

$$\sigma^n = \sigma^u + \Delta\sigma_e. \tag{3.3}$$

2. The new arguments for the yield condition

$$\begin{aligned} \sigma_0 &= \sigma^u - \alpha^u, \\ \sigma_1 &= \sigma^n - \alpha^u. \end{aligned} \tag{3.4}$$

3. The interval $\overline{\varepsilon}^p_k$, $\overline{\varepsilon}^p_{k+1}$ to which our $\overline{\varepsilon}^{pu}$ belongs and the corresponding H^α and H^I, as well as such k that

$$\overline{\varepsilon}^p_k < \overline{\varepsilon}^{pu} < \overline{\varepsilon}^p_{k+1}.$$

4. The actual yield point

$$Y^u = Y(\overline{\varepsilon}^{pu}) = Y_k + H^I_k(\overline{\varepsilon}^{pu} - \overline{\varepsilon}^p_k). \tag{3.5}$$

5. Now we substitute this into the yield point condition

$$\begin{aligned} F_0 &= f(\sigma_0) - Y^u, \\ F_1 &= f(\sigma_1) - Y^u. \end{aligned} \tag{3.6}$$

6. We check whether plastic flow occured in this step, that is if $F_1 > 0$. If not, the present increment is evaluated from the elastic characteristic, that is $\sigma = \sigma^n$. Then we pass to the next increment (that is to the beginning of the algorithm).

7. If $F_1 > 0$, we check whether the material was, in the previous step (previous increment), in a state of plastic flow, that if the relation $F_0 = 0$ was true. If $F_0 < 0$, the material passes in the present step from the elastic state to the plastic state. We calculate the fraction by which the actual increment of the stress exceeds the actual surface of flow. This fraction will be denoted by R,

$$R = \frac{F_1}{F_1 - F_0} \qquad (\text{if} \quad F_0 = 0, \quad R = 1). \tag{3.7}$$

$R\Delta\sigma$ is that part of the stress tensor increment which must be reduced to the yield surface. To this aim $R\Delta\sigma$ is divided into n parts (the number n depending on the required accuracy), and the value of one part is determined from the formula

$$\Delta\sigma = \frac{1}{n} R\Delta\sigma_e. \tag{3.8}$$

The current value of σ_0 is corrected, in agreement with (3.9), to get it located on the yield surface (that is σ_i is assumed as a new σ_0)

$$\sigma_i = \sigma_0 + (1 - R)\Delta\sigma_e. \tag{3.9}$$

Next the fraction $R\Delta\sigma_e$ is reduced in n steps, by performing n times the operations of:

a) determining $\left(\frac{\partial f}{\partial \sigma}\right)_i$, H_i^*, H_i^I for the current σ_i and $\bar{\varepsilon}_i^p$,

b) calculating the vector $\mathbf{d}$ (from (2.18))

$$\mathbf{d} = \mathbf{D} \cdot \frac{\partial f}{\partial \sigma},$$

c) calculating $\Delta\lambda_i$ (from (2.17))

$$\Delta\lambda_i = \frac{\frac{\partial f^T}{\partial \sigma} \cdot \Delta\sigma}{H_i^* + \left(\frac{\partial f^T}{\partial \sigma}\right)_i \cdot \mathbf{d}_i},$$

d) calculating the correct increment of the stress

$$\Delta\sigma_i = \Delta\sigma - \Delta\lambda_i \mathbf{d},$$

e) calculating the corrected values of the quantities connected with the kinematic strain-hardening

$$\Delta\mu_i = \frac{\frac{\partial f^T}{\partial \sigma} \cdot \Delta\sigma_i - H^I \Delta\lambda_i}{\frac{\partial f^T}{\partial \sigma} \cdot \sigma_i},$$

$$\Delta\alpha_i = \Delta\mu_i \sigma_i,$$

$$\alpha_i = \alpha_i + \Delta\alpha_i,$$

$$\Delta\sigma_i = \Delta\sigma_i - \Delta\alpha_i,$$

f) correcting the values of the stress and the plastic strain

$$\sigma_{i+1} = \sigma_i + \Delta\sigma_i,$$

$$\bar{\varepsilon}_{i+1}^p = \bar{\varepsilon}_i^p + \Delta\lambda_i.$$

Finally, the computed values of the stresses are verified for location on the yield surface, that is the relation

$$|f(\sigma_{i+n}) - Y(\bar{\varepsilon}_{i+n}^p)| \leq \sigma^r,$$

is verified for being true, σ_r denoting the assumed value of the admissible error. If this inequality is satisfied, the values of σ_{i+n} and α_{i+n} must be corrected.

The algorithm just presented was used for writing a program based on the method of finite elements, which has already been devised earlier by the present author, especially for problems of stresses in structures with a TSL [5, 6, 11].

4. Analysis of a notched cylindrical element with a TSL, subjected to a cyclic load

The program just mentioned was used to analyse the influence of the surface layer on the strength of the material of a specimen with a circular notch Fig. 3, subjected to a cyclic load.

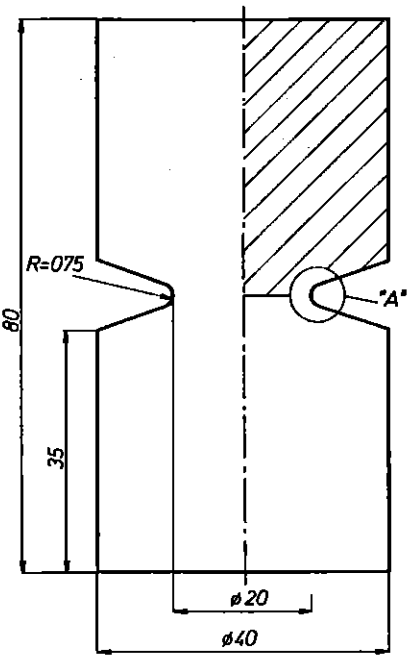

Fig. 3. A cylindrical specimen with a circular notch.

Two specimens have been considered for the sake of comparison, that is a homogeneous specimen and a specimen with a TSL, both specimens being subjected to identical tensile load $p = \mp 75$ MPa. The finite element meshes are illustrated in Fig. 4, showing (in view of the problem being symmetric) only a quarter of the specimen (shaded in Fig. 3).

The surface layer is modelled by membrane elements as described in [6]. Those elements are connected with the remaining elements at nodes which are situated on the surface and are marked, in Fig. 4, with a heavy line. To make the comparison accurate, an identical geometrical model is used for the homogeneous specimen and that with a TSL, which means that the material at the surface is modelled in both cases by membrane elements, the material properties of each of the two membrane being, in the nonhomogenous case, different. The value of the load p is selected to cause partial yielding of the cross-section of the homogeneous specimen to a depth of some 2 mm from

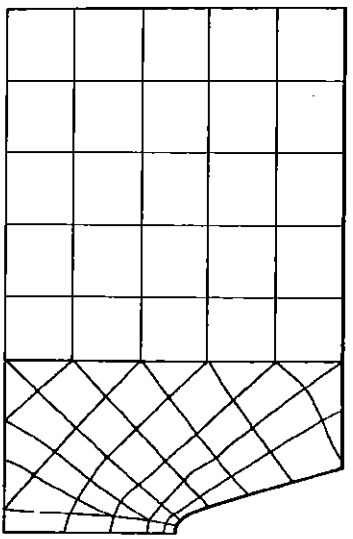

FIG. 4. The FEM.

the surface, at the bottom of the notch. It was assumed that the surface layer of the second specimen has the properties of a burnished layer, that is an elevated yield point $\sigma_e = 800$ MPa and self-stresses $\sigma_\varphi = \sigma_z = -700$ MPa. The thickness of the layer is 0.2 mm. The distribution of the self-stresses σ_z in the initial state (before beginning the loading process) in the section passing through the bottom of the notch, determined from the equilibrium equations, is shown in Fig. 5. The diagram is confined to region on the right-hand side of the symmetry axis.

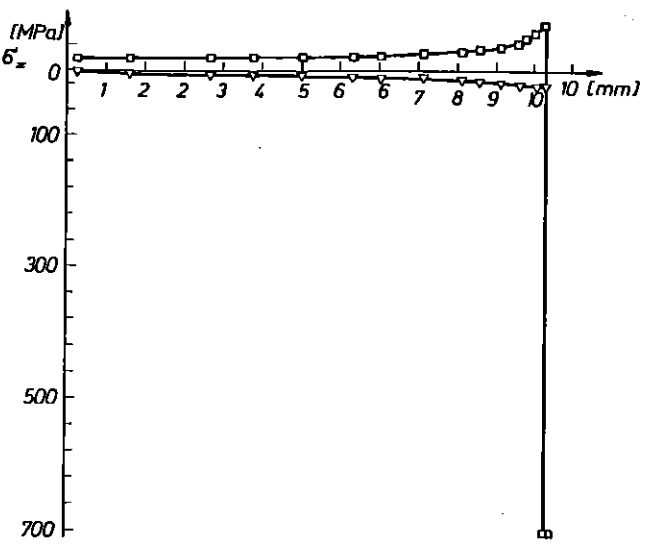

FIG. 5. The initial stresses σ_z in an element with a TSL.

The application of the model described above requires the use of the curves of kinematic and isotropic strain hardening as obtained from the test of uniaxial cyclic load performed for determining the values of the moduli H^{α} and H^{i} in consecutive intervals of $\bar{\varepsilon}^{p}$ (Eq. (3.1)). The results of the tests are most often presented in the form of a stress hysteresis loop, that is the cyclic curve of total strain hardening (H^{*}) and the hysteresis loop of the parametr α, that is the cyclic curve of kinematic strain hardening (H^{α}). The curve of isotropic strain hardening is obtained by subtracting from the coordinate of the total strain-hardening curve, the corresponding ordinates of that of kinematic strain hardening. The curves which were used for the analysis are presented in Figs. 6 and 7. They are close to those obtained from experiments [9], Fig. 1. Compared with the experimental curves, they show a small modification consisting chiefly in a variation in inclination angle of the curve of isotropic strain hardening so that it represents a constant value for smaller $\bar{\varepsilon}^{p}$ than in the reality. This does not influence the aim of the analysis but makes possible a reduction of the necessary time.

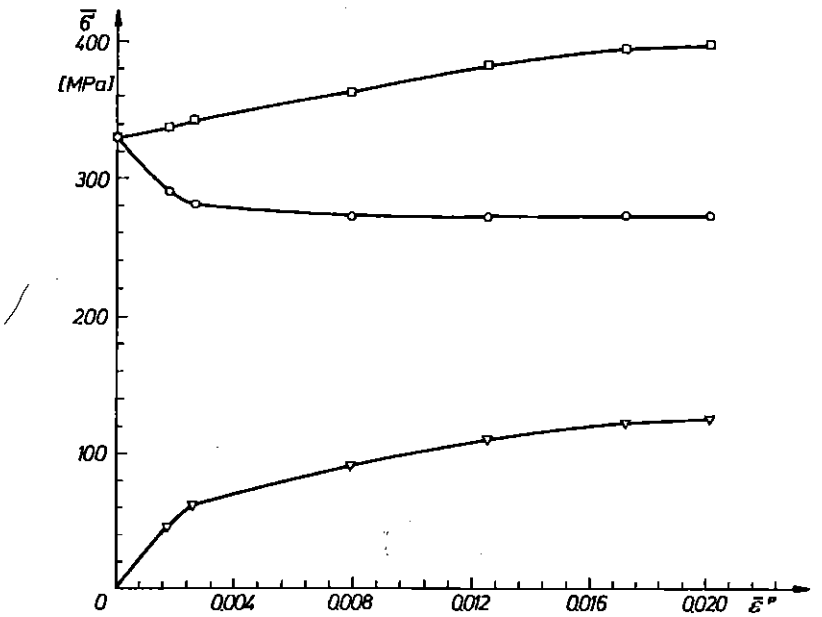

FIG. 6. The characteristics assumed for monotonic tension ▽ curve of kinematic strain hardening, o curve of isotropic strain hardening, □ curve of total strain hardening.

As a result of computation, we obtain for consecutive increments of load the values of all the components of the stress tensor, as functions of $\bar{\varepsilon}^{p}$, at every Gauss point, therefore we are able to determine their hysteresis loops. Presentation of the results in the form of a hysteresis loop of effective

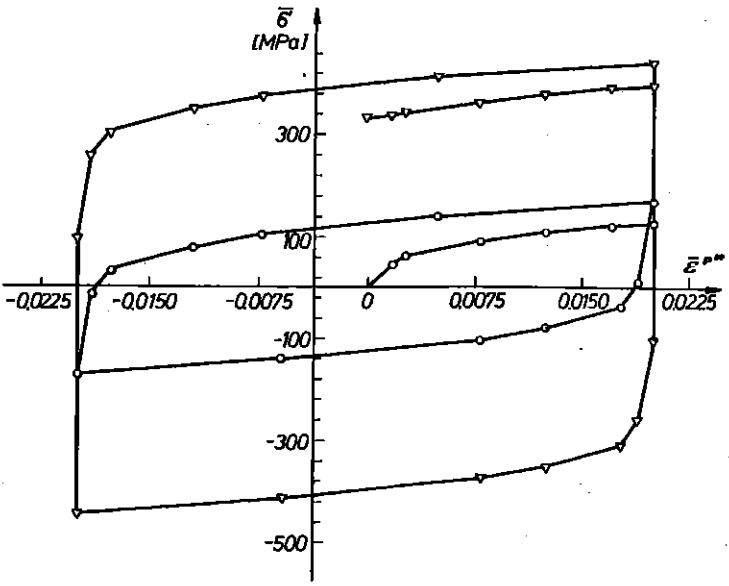

FIG. 7. The assumed cyclic curves of strain hardening; ∇ total, o kinematic.

stress seems to be most useful, however, for making it possible to compare the multiaxial state of stress in the notch (in which we are interested) with the uniaxial state occurring during tension tests, which are performed for determining the characteristics of the material. Such a presentation of the results requires special processing, which is somewhat inconvenient, it being required to change the signs of the reduced stress and $\bar{\varepsilon}^p$, but enables us to state easily whether the process has become stable, that is whether the loops are closed. As regards the cause of destruction of a specimen, the hysteresis loops for the points A and B, which are located near the bottom of the notch (Fig. 8), are the most interesting. In the case of a nonhomogeneous specimen the point B is located within the region of the layer.

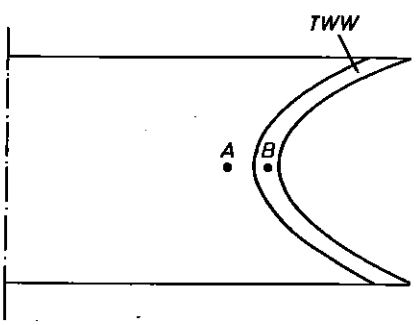

FIG. 8. The points for which the hysteresis loops of effective stress are determined (part A of Fig. 3).

Figure 9 shows the hysteresis loops at the point A for a specimen with and without the layer. Comparison between the hysteresis loops at the point B with and wihout a surface layer is illustrated in Fig. 10.

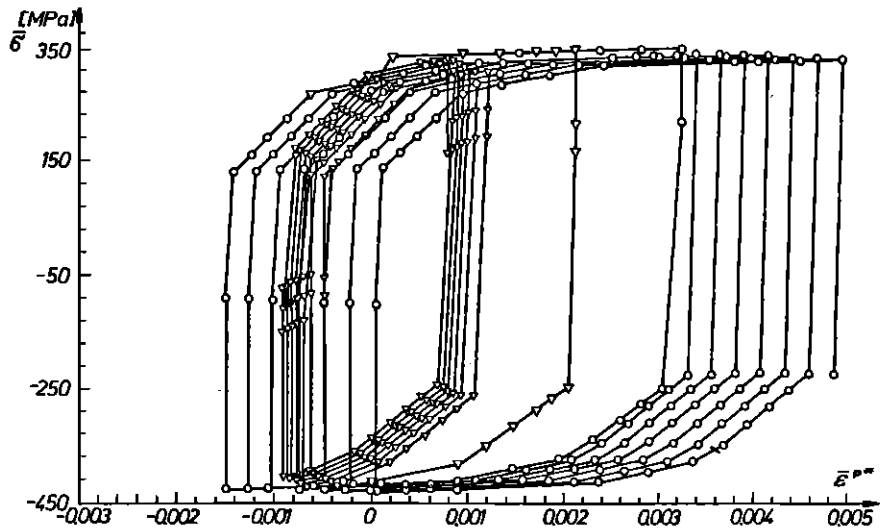

FIG. 9. The hysteresis loops at the point A; ∇ for the specimen with a layer, o for the specimen without a layer.

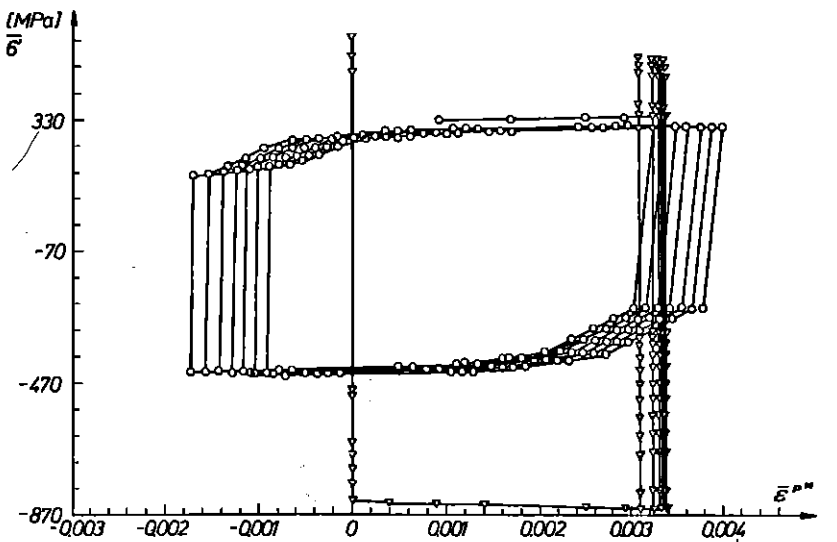

FIG. 10. The hysteresis loops at the point B; ∇ for the specimen with a layer, o for the specimen wihout a layer.

Another interesting problem is that of evolution of the state of residual stress. It should be borne in mind that the residual stress after a cycle

constitutes the initial self-stress for the next cycle. Moreover, for an assumed value of the load (which produces partial plasticity), residual stresses occur in the case of a homogeneous specimen and a specimen with a TSL as well. After the hysteresis loop has become stable, the distribution of the residual stress depends in both cases on whether the load cycle ends with

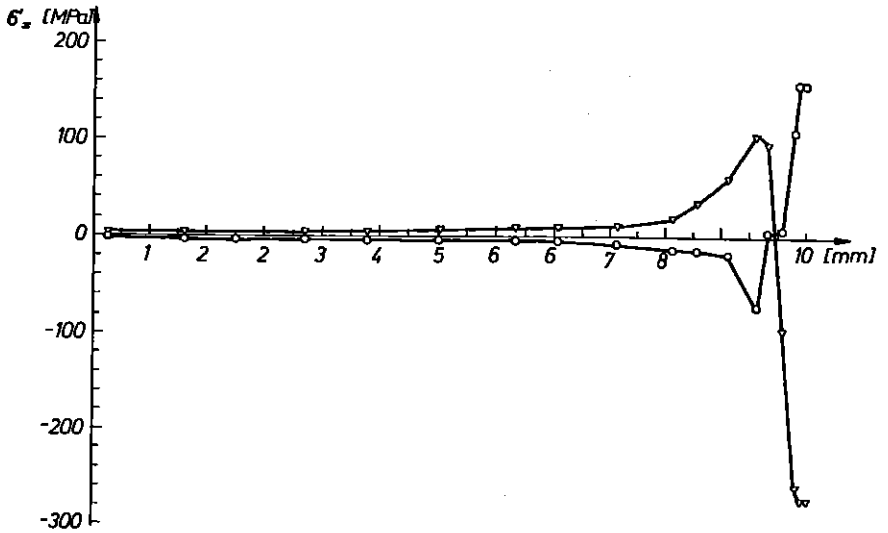

FIG. 11. Residual stress σ_z in the homogeneous specimen o load cycle ending with $-p$, ∇ load cycle with $+p$.

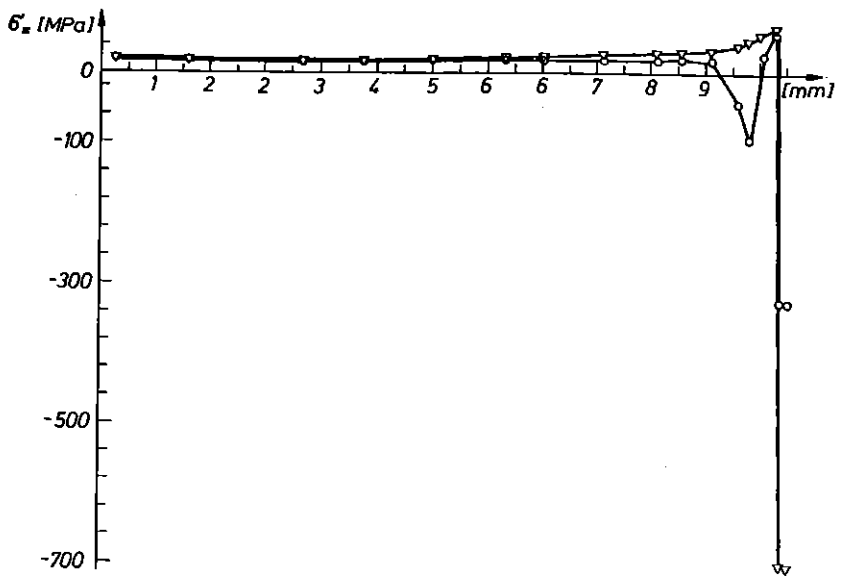

FIG. 12. Residual stress σ_z in the specimen with a TSL ∇ technological (initial) stress, o afer a load cycle ending with $-p$.

$+p$ or $-p$. Relevant diagrams are represented in Fig. 11 for the homogeneous specimen and in Figs. 12 and 13 for the specimen with a TSL. Diagrams of technological initial stresses are shown for comparison, on the same figures, for the specimen with a TSL.

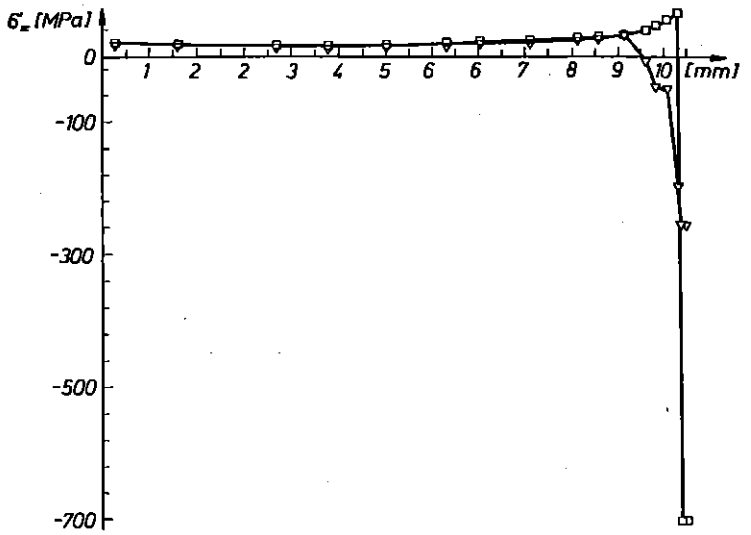

FIG. 13. Residual stress σ_z in the specimen with a TSL □ technological (initial) stress, ▽ afer a cycle ending with $+p$.

5. INFERENCES

The surface layer has a considerable influence on the behaviour of the material at the bottom of a notch of a specimen subjected to a cyclic load. Initial stresses introduced by technological means into the TSL makes the state of residual stress after the load cycle has ended, different from the state in the homogeneous specimen. This modification does not concern the surface layer alone, but also the material in the region located below the layer. Moreover, the initial stress is considerably modified already after no more than a few load cycles (cf. Figs. 12 and 13). By confronting the hysteresis loops for a specimen with and wihout a layer at the point A, Fig. 9, it is seen that they are characterized by roughly the same stress amplitude and the same limiting values of the stresses (for compression and tension, respectively), but the area of the hysteresis loop is much greater in the case of a specimen without surface layer.

As regards the hysteresis loop at the point B, Fig. 10, its form is, in the case of presence of a TSL, degenerate. There occur high stresses, but in view of the existence of the self-stresses the material at that point is plastified

only in the case of compression, but the area of the hysteresis loop is zero. In the case of a homogeneous specimen the values of the stress are lower, but the area of the loop is different from zero.

The area of the hysteresis loop is a measure of the energy dissipated per one load cycle and influencing in turn the fatigue life of the specimen. Comparison between the hysteresis loops for a specimen with and whithout a surface layer enables us to explain the experimental fact that the existence of that layer influences little the strength of the specimen in the case of a monotonic loading, its influence being considerable for the fatigue strength, however. In the case of a monotonic load, for which the strength depends on the value of the stress, the results of computation show that the difference between a homogeneous specimen and a specimen with a TSL is practically confined to that layer, which is a simple consequence of the yield point having been raised. In the case of a cyclic load, the strength is decided upon by the areas of the hysteresis lopps which are, for a homogeneous specimen, greater for both the surface layer (point B, Fig. 8) and the region below the surface layer (point A, Fig. 8). Thus, in the case of a monotonic loading, the influence of the surface layer is limited in principle to its region, but in the case of a cyclic load its influence range is extended to the material in direct neighbourhood of the surface layer.

During the experimental investigation it was also observed that the destruction of an element with a TSL begins sometimes under the layer. The results of computation explain this observation, because in our case the hysteresis loop of the material under the layer has a much larger area than in the layer.

By analysing the hysteresis loops obtained for a specimen with a TSL (Figs. 9 and 10) it is seen that in the core, under the layer, we are concerned with cyclic stressing of the material. There occur in that region hysteresis loops of non-zero area, the form of which results from the isotropic and kinematic strain hardening. As regards the surface layer, the loops are asymmetric, their area is zero and there occurs a phenomenon of shakedown. To find optimum parameters for the TSL by using the above program it is necessary to complete the latter with some fatigue criteria, in agreement with the types of stressing of the material mentioned above. This will be the subject of further attempts.

References

1. K. Komvopoulos, *Finite element analysis of a layered elastic solid in normal contact with a rigid surface*, ASME J. Tribology, **110**, 477–485, 1988.

2. O. SATOSHI and M. KOUITSU, *Residual stress calculation of case hardened thin-rimmed spur gears with various standard pressure angles*, The Third Intern. Conference on Residual Stresses, ICRS-3, Tokushima, Japan, 1991.

3. P. MONTMITONNET, M.L. EDLINGER and E. FELDER, *Finite element analysis of elastoplastic indentation. Part II. Application to hard coatings*, J. Tribology, **115**, 15–19, 1993.

4. Z. MRÓZ and G. STARZYŃSKI, *An elasto-plastic analysis of a cylinder with surface layer under cyclic loading*, Arch. Machine Design, 1994.

5. Z. HANDZEL-POWIERŻA, S. KUCHARSKI, G. STARZYŃSKI and M. DĄBROWSKI, *New methods for determining the stress fields in elements with a technological surface layer, subjected to elastic-plastic strain* [in Polish], Zesz. Nauk. PW, Warszawa 1990.

6. Z. HANDZEL-POWIERŻA and S. KUCHARSKI, *Determination of stresses in structure with TSL by the method of finite element* [in Polish], Engng. Trans., **38**, 3-4, 635–647, 1990.

7. J. SKRZYPEK, *Plasticity and creep. Theory. Applications. Problems* [in Polish], PWN, Warszawa 1986.

8. Z. MRÓZ, *Phenomenological constitutive models for metals*, [in:] Modelling of small deformations of polycrystals, J. ZARKA [Ed.], Elsevier Appl.Sci., 1986.

9. W. TRĄMPCZYŃSKI, *A study of the influnce of the history of loading on the phenomenon of creep of metals in a complex state of stress* [in Polish], Prace IPPT, 36, 1985.

10. D.R.J. OWEN and E. HINTON, *Finite element in plasticity. Theory and practice*, Pineridge Press Ltd., Swansea 1980.

11. S. KUCHARSKI, *The use of the transitional elements for stress analysis of structures with a technological surface layer by the method of finite elements*, Engng. Trans., **42**, 1-2, 1994.

POLISH ACADEMY OF SCIENCES
INSTITUTE OF FUNDAMENTAL TECHNOLOGICAL RESEARCH.

Received March 29, 1995.